were recorded in $CHCl_3$, $CDCl_3$, or C_6H_6 and referenced to a 1% H_3PO_4 (0.0 ppm) external secondary reference. A low-field positive chemical shift convention is used in reporting data. In all cases a 10-mm variable-frequency probe was used.

Low-temperature experiments were conducted on the NR-80B using a variable-temperature unit. A nitrogen gas flow, from liquid nitrogen, was passed over a resistance heater and used to obtain the required temperature with a stability of ±0.5 K by use of a thermocouple-regulated temperature-control unit. The temperature reading was calibrated with a low-temperature thermometer held in a $CHCl_3$-filled NMR tube by a septum and read after reaching thermal equilibrium in the probe. Temperature calibration was made after the data collection was concluded for a given temperature.

Infrared spectra were collected by using KBr pellets on Perkin-Elmer 283B and Beckman IR 4250 spectrophotometers. Calibration used polystyrene and carbon monoxide.

Reaction of $IrCl(CO)(PPh_3)_2$ with Cl_2SO at 263 K. A 0.2-g sample of **1** was dissolved in 10 mL of $CDCl_3$, and 5 mL of solution was transferred to a 10-mm NMR tube capped with a rubber septum. The sample was held at 263 K by a constant-temperature bath. A solution of 1:3 Cl_2SO in $CDCl_3$ was prepared, and additions of the Cl_2SO solution were made into the NMR tube through the septum via a syringe. Additions were made so as to obtain the $IrCl(CO)(PPh_3)_2$ to Cl_2SO ratios shown in Figure 1. The solution was rapidly mixed by inverting the tube and then was returned to the low-temperature bath. The sample was taken to the spectrometer in the low-temperature bath and placed into the 263 K NMR probe. Further aliquots of Cl_2SO and **1** were added with the same technique.

Attempts To Isolate the Green Intermediate in the Title Reaction. An experimental procedure for the preparation of $IrCl_2(CO)(PPh_3)_2(SOCl)$[6] was followed, except that the amount of Cl_2SO used was reduced to $^1/_2$ equiv. The mixing of 0.616 g (0.789 mmol) of $IrCl(CO)(PPh_3)_2$ and 0.029 mL (0.40 mmol) of Cl_2SO in benzene gave an emerald green solution. Reduction of the volume by pumping off some of the benzene resulted in the precipitation of an orange solid and left a yellow-orange solution. A hexane precipitation of the filtrate yielded a yellow solid. By infrared spectroscopy, both solids were mixtures of $IrCl_2(CO)(PPh_3)_2(SOCl)$ and $IrCl(CO)(PPh_3)_2$. Other attempts at precipitation or evaporation invariably led to yellow or orange products and disappearance of the green color.

Variable-Temperature Study of $IrCl(CO)(PPh_3)_2$ and $IrCl(CO)(PPh_3)_2(SO_2)$. A sample was prepared under a nitrogen atmosphere in chloroform having equal concentrations of **1** and **5** (0.05 M in each complex). ^{31}P NMR spectra were collected from 213 to 303 K, and nine points from 240.2 to 267.6 K were used in the analysis. For each temperature the mixture of **1** and **5** was allowed to reach thermal equilibrium in the probe (~15 min for small temperature changes) after which FIDs were collected and stored on disk. A sample of **1** (0.05 M in chloroform) was next allowed to equilibrate in the probe and its FID stored. Finally, the temperature was determined as described above.

Experimental spectra for temperatures 240.2, 243.0, 247.0, 250.0, 253.0, 257.0, 260.0, 265.0, and 270.0 K were hand-digitized and subjected to a complete band shape analysis as described by Sandström.[21] The shape function[22] for a noncoupled, equal-population, two-site exchange was used in the nonlinear least-squares program NLLSQ.[23] Nonexchange bandwidths were determined on **1** over the experimental temperature range. It was assumed that the nonexchange bandwidth for **5** was the same as for **1**. The NLLSQ fit parameters were used to calculate a value for the exchange lifetime, τ, for each spectrum. The activation parameters ΔH^{*} and ΔS^{*} were then calculated[21] from a plot of ln $(1/T\tau)$ vs. $1/T$. The linear least-squares analysis of this plot using the program LINGEN[24] used weighted values for both x and y.

Acknowledgment. Partial support for this work was provided by the donors of the Petroleum Research Fund, administered by the American Chemical Society, and the Research Corp. We thank Dr. B. M. Fung for his help on the band shape analysis.

Registry No. **1**, 15318-31-7; **2**, 59599-05-2; **3a**, 22788-78-9; **3b**, 24810-96-6; **4**, 26545-07-3; **5**, 15692-64-5; Cl_2SO, 7719-09-7; $IrCl(CO)(PPh_3)_2(O_2)$, 15187-10-7.

---

(21) Sandström, J., "Dynamic NMR Spectroscopy"; Academic Press: New York, 1982.

(22) Williams, K. C.; Brown, T. L. *J. Am. Chem. Soc.* **1966**, *88*, 4134–4140.

(23) The program is a local modification by B. M. Fung of the general nonlinear least-squares program NLLSQ written in Apple Basic (Christian, S. D.; Tucker, E. E. *Am. Lab.* (*Fairfield, Conn.*) **1982**, *14* (9), 31–36).

(24) Christian, S. D.; Tucker, E. E. *J. Chem. Educ.* **1984**, *61*, 788.

Contribution from the Department of Chemistry,
University of Calgary, Calgary, Alberta, Canada T2N 1N4

Reactions of Hydride with Tungsten Complexes Containing Organosulfur Ligands: Synthesis and Characterization of (μ-Hydrido)bis(μ-dimethyl sulfide)ditungsten(III) Species[1]

P. MICHAEL BOORMAN,* KELLY J. MOYNIHAN, VIKRAM D. PATEL, and JOHN F. RICHARDSON

Received December 11, 1984

The reaction between $WCl_4(Me_2S)_2$ and an excess of Et_3SiH in CH_2Cl_2 solution was found to produce HCl, H_2, and trace quantities of CH_4; the major tungsten-containing product was identified as the diamagnetic, ditungsten(III) hydrido complex, $Cl_3W(\mu\text{-}H)(\mu\text{-}Me_2S)_2WCl_2(Me_2S)$ (**1**). X-ray crystallographic analysis of a chloroanionic derivative of **1**, $[Ph_4P][Cl_3W(\mu\text{-}H)(\mu\text{-}Me_2S)_2WCl_3]\cdot 2CH_2Cl_2$, revealed that this series of dinuclear compounds possesses a confacial bioctahedral framework distorted by a strong W–W (≈triple) bond. The tetraphenylphosphonium salt crystallizes in the triclinic space group $P\bar{1}$, with $a = 11.620$ (2) Å, $b = 12.841$ (2) Å, $c = 14.667$ (2) Å, $\alpha = 79.45$ (1)°, $\beta = 81.17$ (1)°, $\gamma = 76.45$ (1)°, and $Z = 2$. The structure refined to $R = 0.039$ and $R_w = 0.037$ based on 3413 observed data. The position of the μ-H atom was located in the difference map, but could not be successfully refined. The presence of the hydride ligand is confirmed by infrared and NMR spectroscopic results, including data for corresponding deuterio derivatives for comparison. The ^1H NMR signal for the μ-H in these complexes was observed at relatively low field (δ ~3.7), and this chemical shift was observed to vary in an unusual manner with temperature, moving upfield as the temperature is lowered. Spin coupling between the hydride ligand and ^{183}W nuclei remains constant, with $J(^{183}W-^1H) = 110 \pm 3$ Hz, over the temperature range −80 to +22 °C. The ^1H NMR spectrum of the neutral complex **1**, over the temperature range −70 to +20 °C, is interpreted on the basis of the existence of a C_s isomer and an enantiomeric pair of C_1 isomers. With increasing temperature the enantiomers interconvert, through a process believed to involve the exchange of two Me_2S ligands between terminal and bridging sites.

Introduction

The activation of C–S bonds in organosulfur species toward cleavage upon coordination of the sulfur atom to a metal center is a topic of potential relevance to the process of catalytic hydrodesulfurization. Most of the mechanisms proposed for this process assume that in the activation of H_2 to enable the hydrogenolysis of the C–S bond, the hydrogen is provided by S–H groups on the metal sulfide catalyst surface.[2,3] Rakowski Dubois

---

(1) Taken in part from: Moynihan, K. J. Ph.D. Thesis, University of Calgary, 1983.

(2) (a) Massoth, F. E.; Kirby, C. L. *J. Catal.* **1977**, *47*, 300. (b) Massoth, F. E. *J. Catal.* **1977**, *47*, 316.

0020-1669/85/1324-2989$01.50/0

et al.[4] have been able to model the reaction of H_2 with sulfide ligands, as is required in the above mechanism, by demonstrating that several cyclopentadienylmolybdenum complexes, such as $[(CH_3C_5H_4)MoS_2]_2$, will cleave molecular H_2 to form the corresponding hydrosulfido complex, viz. $[(CH_3C_5H_4)Mo(S)SH]_2$. While there can be little doubt that S–H groups play an essential role in the hydrodesulfurization process, the possible involvement of M–H moieties on catalyst surfaces would not seem unlikely. In support of this, evidence as to the nature of hydrogen taken up by MoS_2 has been obtained from inelastic neutron scattering studies.[5] An unexplained band at 872 cm^{-1} was tentatively assigned to Mo–H vibrations. It has been suggested by Chisholm[6] that metal–hydrogen bonds are also likely to be implicated in some of the important catalytic uses of metal oxides.

Very recently this hypothesis has received significant support from the work of Angelici et al.,[7] who demonstrated that π-bonded thiophene will react with nucleophiles, and in particular with hydride, which can be followed by protonation to produce 2,3-dihydrothiophene. For this mechanism to be relevant to the catalytic hydrodesulfurization of thiophene, both hydridic and protonic hydrogen would be needed on a catalytic surface. Following the possible saturation of the thiophene ring, the mode of coordination to the surface of the catalyst would be via sulfur, whereupon the hydrogenolysis of C–S bonds would be required.

The observation in our laboratories[8] that the elimination of RCl from $WCl_5(SR)$ can occur via a carbonium ion mechanism led us to speculate on the possibility of inducing the loss of RH from complexes of molybdenum- or tungsten-containing MH(SR) or $MH(SR_2)$ moieties:

$$MH(SR) \rightarrow MS + RH$$

$$MH(SR_2) \rightarrow M(SR) + RH$$

Adams and co-workers have shown that it is possible to obtain benzene as a degradation product of the thermolysis[9] or photolysis[10] of Os_3 clusters containing hydride and –SPh ligands. If the generality of such processes could be demonstrated, it would lend support to the possible involvement of hydride in one of the steps in catalytic hydrodesulfurization on transition-metal sulfide surfaces.

We have been interested in the possible participation of metal hydrides in hydrodesulfurization, and in this paper we describe the reactions of hydride with various tungsten–sulfur systems. While our attempts to achieve the original objectives were only partially successful, the study led to the synthesis of a series of novel hydride- and thioether-bridged ditungsten(III) complexes. A preliminary account describing some of this work has appeared.[11]

Results

Synthetic and Structural Results. The C–S bond activation observed by Boorman and O'Dell[8] involved the species $WCl_5(SR)$, and hence our first experiments, which were undertaken to find an appropriate source of hydride, involved the compounds $WCl_5(SR)$ as starting materials. Although direct reactions of compounds of this type with hydrogen were attempted, no conclusive results were obtained. Hence we sought an alternative reagent by which hydride could be introduced into the coordination sphere of the metal. That ultimately selected was triethylsilane (Et_3SiH), which, it has been noted,[12] often parallels molecular hydrogen in its reactions with transition-metal complexes. It is experimentally safer than H_2 and, in metathetical reactions with W–Cl bonds, proved to be very convenient since ^1H NMR could be used to monitor the progress of the reactions.

In the reaction of $WCl_5(SR)$ (R = Me, Et, Ph) with 1 molar equiv of Et_3SiH in CH_2Cl_2 solution, an instantaneous reaction occurred in which a gas was evolved and an amorphous rust-colored solid precipitated. The evolved gas proved not to be RH as was hoped, but rather HCl. On the basis of analytical and infrared spectroscopic data the solid was formulated as $[WCl_3(SR)]_n$. Its insolubility suggested it to be a polymeric material for which a structure similar to that of WCl_4 would be plausible.[13] Such species do not appear to have been described previously. The reaction can be written as

$$WCl_5(SR) + Et_3SiH \rightarrow WCl_4H(SR) + Et_3SiCl$$

$$WCl_4H(SR) \rightarrow [WCl_3(SR)]_n + HCl$$

Clearly the oxidizing properties of the W(VI) center are too strong to enable the alternative reaction, viz. $WCl_4(H)SR \rightarrow WCl_4S + RH$, to occur. We therefore turned our attention to a less oxidizing system, namely one involving a W(IV) center. In the light of previous work in this laboratory, it was decided to use the compound $WCl_4(Me_2S)_2$ as a starting material. This very reactive compound is conveniently prepared and handled and contains one of the target moieties for our study, a coordinated thioether.

Upon reaction of $WCl_4(Me_2S)_2$ with a minimum of 3 mol of Et_3SiH (excess of the silane was found to be required for the reaction), the CH_2Cl_2 solution darkened in color and over ~20 h a purple, amorphous solid precipitated. Monitoring of the gaseous phase above the solution indicated that during the reaction significant quantities of H_2 and HCl were evolved together with trace quantities of methane. By the use of Et_3SiD instead of Et_3SiH in this reaction, it was confirmed that the methane originated from a hydride ligand, which was introduced into the tungsten coordination sphere of the starting material, and from a methyl group derived from a coordinated $(CH_3)_2S$, since CH_3D was then found to be evolved. Thus it appeared that the original hypothesis was not entirely without foundation. Unfortunately, no tungsten-containing product resulting from a methane-liberating process could be isolated from the reaction mixture. The focus of subsequent research on this reaction therefore turned to the identity of the purple solid and its derivatives.

The $WCl_4(Me_2S)_2/Et_3SiH$ reaction yields, as its major solid product, the novel ditungsten(III) complex $Cl_3W(\mu\text{-}H)(\mu\text{-}Me_2S)_2WCl_2(Me_2S)$ (**1**). Feasible reactions that might produce this compound are shown in Scheme I. Reactions 2 and 4 imply an intermolecular reductive elimination of HCl or H_2, but it is easy to postulate analogous reactions involving intramolecular loss of HCl or H_2, followed by coordination of a W(IV) to a W(II) moiety.

Scheme I

$$WCl_4(Me_2S)_2 + Et_3SiH \rightarrow WCl_3H(Me_2S)_2 + Et_3SiCl \quad (1)$$

$$2WCl_3H(Me_2S)_2 \rightarrow Cl_3W(\mu\text{-}H)(\mu\text{-}Me_2S)_2WCl_2(Me_2S) + HCl + Me_2S \quad (2)$$

and/or

$$WCl_3H(Me_2S)_2 + Et_3SiH \rightarrow WCl_2H_2(Me_2S)_2 + Et_3SiCl \quad (3)$$

$$WCl_3H(Me_2S)_2 + WCl_2H_2(Me_2S)_2 \rightarrow Cl_3W(\mu\text{-}H)(\mu\text{-}Me_2S)_2WCl_2(Me_2S) + H_2 + Me_2S \quad (4)$$

Although numerous attempts were made to crystallize **1**, these were without avail. Spectroscopic evidence suggested the presence of terminally ligated dimethyl sulfide in the compound, and hence the possibility of obtaining a crystalline derivative by displacing this labile ligand suggested itself.[14] The first crystalline com-

---

(3) Kwart, H.; Schuit, G. C. A.; Gates, B. C. *J. Catal.* **1980**, *61*, 128.

(4) Rakowski Dubois, M.; Van Derveer, M. C.; Dubois, D. L.; Haltiwanger, R. C.; Miller, W. K. *J. Am. Chem. Soc.* **1980**, *102*, 7456.

(5) Vasudevan, S.; Thomas, J. M.; Wright, C. J.; Sampson, C. *J. Chem. Soc., Chem. Commun.* **1982**, 418.

(6) Chisholm, M. H.; Folting, K.; Huffman, J. C.; Rothwell, I. P. *J. Am. Chem. Soc.* **1982**, *104*, 4389.

(7) Lesch, D. A.; Richardson, J. W.; Jacobson, R. W.; Angelici, R. J. *J. Am. Chem. Soc.* **1984**, *106*, 2901.

(8) Boorman, P. M.; O'Dell, B. D. *J. Chem. Soc., Dalton Trans.* **1980**, 257.

(9) Adams, R. D.; Katahira, D. A.; Yang, L-W. *Organometallics* **1982**, *1*, 235.

(10) Adams, R. D.; Horvāth, I. T.; Kim, H.-S. *Organometallics* **1983**, *3*, 548.

(11) Boorman, P. M.; Moynihan, K. J.; Kerr, K. A. *J. Chem. Soc., Chem. Commun.* **1981**, 1286.

(12) Murai, S.; Sonoda, N. *Angew. Chem., Int. Ed. Engl.* **1979**, *18*, 837.

(13) Schnering, H. G.; Wohrle, H. *Angew. Chem., Int. Ed. Engl.* **1963**, *2*, 558.

(14) Patel, V. D.; Boorman, P. M. *Can. J. Chem.* **1982**, *60*, 1339.

Table I. Atomic Positional Parameters ($\times 10^4$; $\times 10^3$ for C) for the Non-Hydrogen Atoms of the Anion $[Cl_3W(\mu\text{-}H)(\mu\text{-}Me_2S)_2WCl_3]^-$ [a]

atom	*x*/*a*	*y*/*b*	*z*/*c*
W(1)	2580.6 (7)	2607.9 (6)	801.2 (5)
W(2)	1715.3 (7)	2097.0 (6)	2381.9 (6)
Cl(1)	1667 (4)	2936 (4)	−641 (3)
Cl(2)	4389 (4)	1517 (4)	171 (4)
Cl(3)	3464 (4)	4147 (4)	411 (4)
Cl(4)	−279 (4)	1815 (4)	2861 (3)
Cl(5)	2634 (5)	510 (4)	3340 (4)
Cl(6)	1734 (4)	3129 (4)	3567 (3)
S(1)	1834 (4)	995 (4)	1211 (3)
S(2)	872 (4)	3769 (4)	1475 (3)
C(1)	279 (2)	−31 (1)	126 (1)
C(2)	55 (1)	77 (1)	79 (1)
C(3)	97 (2)	504 (1)	179 (1)
C(4)	−62 (1)	398 (1)	111 (1)
H(1)[b]	3117	2136	1674

[a] Esd's are given in parentheses. [b] H(1) positional parameters were not refined.

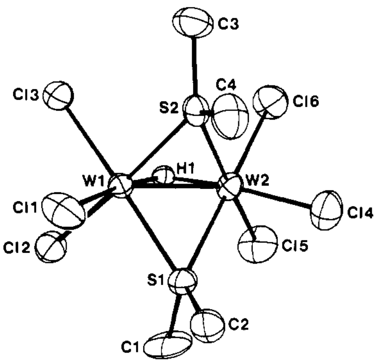

Figure 1. ORTEP plot of the anion in the complex $[Ph_4P][Cl_3W(\mu\text{-}H)(\mu\text{-}Me_2S)_2WCl_3]\cdot 2CH_2Cl_2$ displaying the thermal ellipsoids at 50% probability and showing the atomic numbering scheme.

Table II. Bond Distances (Å) and Angles (deg)[a] for the Anion $[Cl_3W(\mu\text{-}H)(\mu\text{-}Me_2S)_2WCl_3]^-$

	Distances		
W(1)–W(2)	2.419 (1)		
W(1)–H(1)	1.48	W(2)–H(1)	1.80
W(1)–S(1)	2.372 (5)	W(2)–S(1)	2.386 (5)
W(1)–S(2)	2.386 (4)	W(2)–S(2)	2.389 (4)
W(1)–Cl(1)	2.435 (5)	W(2)–Cl(4)	2.407 (5)
W(1)–Cl(2)	2.394 (4)	W(2)–Cl(5)	2.378 (5)
W(1)–Cl(3)	2.375 (5)	W(2)–Cl(6)	2.376 (6)
S(1)–C(1)	1.78 (2)	S(2)–C(3)	1.800 (2)
S(1)–C(2)	1.80 (2)	S(2)–C(4)	1.841 (2)
	Angles		
W(1)–H(1)–W(2)	94.7		
W(1)–S(1)–W(2)	61.1 (1)	W(1)–S(2)–W(2)	60.9 (1)
H(1)–W(1)–S(1)	79.5	H(1)–W(2)–S(1)	73.8
H(1)–W(1)–S(2)	97.1	H(1)–W(2)–S(2)	88.7
S(1)–W(1)–S(2)	96.4 (2)	S(1)–W(2)–S(2)	96.0 (2)
H(1)–W(1)–Cl(1)	166.1	H(1)–W(2)–Cl(4)	160.0
H(1)–W(1)–Cl(2)	80.7	H(1)–W(2)–Cl(5)	90.0
H(1)–W(1)–Cl(3)	97.8	H(1)–W(2)–Cl(6)	103.6
S(1)–W(1)–Cl(1)	87.6 (2)	S(1)–W(2)–Cl(4)	87.0 (2)
S(1)–W(1)–Cl(2)	87.0 (2)	S(1)–W(2)–Cl(5)	87.7 (2)
S(1)–W(1)–Cl(3)	175.9 (2)	S(1)–W(2)–Cl(6)	176.0 (2)
S(2)–W(1)–Cl(1)	89.4 (2)	S(2)–W(2)–Cl(4)	87.9 (2)
S(2)–W(1)–Cl(2)	175.9 (2)	S(2)–W(2)–Cl(5)	175.5 (2)
S(2)–W(1)–Cl(3)	86.8 (2)	S(2)–W(2)–Cl(6)	86.8 (2)
Cl(1)–W(1)–Cl(2)	93.7 (2)	Cl(4)–W(2)–Cl(5)	94.7 (2)
Cl(1)–W(1)–Cl(3)	94.8 (2)	Cl(4)–W(2)–Cl(6)	95.9 (2)
Cl(2)–W(1)–Cl(3)	89.6 (2)	Cl(5)–W(2)–Cl(6)	89.3 (2)
W(1)–S(1)–C(1)	121.9 (7)	W(2)–S(1)–C(1)	121.3 (7)
W(1)–S(1)–C(2)	125.1 (6)	W(2)–S(1)–C(2)	123.7 (6)
W(1)–S(2)–C(3)	121.3 (6)	W(2)–S(2)–C(3)	120.0 (6)
W(1)–S(2)–C(4)	123.2 (7)	W(2)–S(2)–C(4)	120.5 (6)
C(1)–S(1)–C(2)	101.5 (9)	C(3)–S(2)–C(4)	106.0 (8)

[a] Quantities involving H(1) do not have an esd as the positional parameters for H(1) were not refined.

Table III. Crystallographic Parameters for **3**

formula	$C_{30}H_{37}S_2Cl_{10}W_2P$
fw	1215.0
space group	$P\bar{1}$
a, Å	11.620 (2)
b, Å	12.841 (2)
c, Å	14.667 (2)
α, deg	79.45 (1)
β, deg	81.17 (1)
γ, deg	76.45 (1)
vol, Å^3	2078 (1)
Z	2
D_c, g cm^{-3}	1.94
cryst description	burgundy plates
radiation	Mo Kα (λ = 0.70926 Å)
temp, K	295 (1)
max θ, deg	24
scan range (Δw), deg	1.5 (0.60 + 0.347 tan θ)
octants collcd	$\pm h,\pm k,+l$
cryst dimens, mm	0.13 × 0.12 × 0.06
boundary planes	7; {010}, {001}, (101), (111), $(\overline{212})$
μ(Mo Kα), cm^{-1}	66.45
min/max transmissn factors	0.248/0.296
no. of unique data	6432
no. of obsd data ($I > 3\sigma(I)$)	3413
R, R_w[a]	0.039, 0.037
GOF	1.10

[a] $R = \sum(||F_o| - |F_c||)/\sum(|F_o|)$; $R_w = [\sum w(|F_o| - |F_c|)^2/\sum w|F_o|^2]^{1/2}$.

pounds prepared were from reactions between **1** and Ph_3P and PPN^+Cl^-, respectively (PPN = bis(triphenylphosphine)nitrogen(1+)). The product crystallized from the reaction of **1** with Ph_3P in $CHCl_3$/hexane solution was $[Ph_3PH][Cl_3W(\mu\text{-}H)(\mu\text{-}Me_2S)_2WCl_3]$ (**2**) rather than the neutral derivative $Cl_3W(\mu\text{-}H)(\mu\text{-}Me_2S)_2WCl_2(PPh_3)$, which was anticipated. Its crystal structure, described earlier,[11] revealed that the $[Cl_3W(\mu\text{-}H)(\mu\text{-}Me_2S)_2WCl_3]^-$ anion possesses (apparently) a confacial bioctahedral framework with a relatively short W–W distance of 2.410 (7) Å, (≈W–W triple bond). The quality of the crystals, and hence of the data set, did not enable us to locate the μ-hydrido ligand, but it was clear from the spectral data (vide infra), and from the heavy-atom framework, that it should be present in the vacant third confacial bioctahedral bridging position. We therefore searched for a more tractable derivative since the PPN^+ salt also gave crystals of poor quality.[15] The solvated Ph_4P^+ salt, $[Ph_4P][Cl_3W(\mu\text{-}H)(\mu\text{-}Me_2S)_2WCl_3]\cdot 2CH_2Cl_2$ (**3**) yielded a data set of sufficiently good quality at 295 K to provide a structural solution in which the hydride ligand could be located. No improvement was made by collecting the data at 173 K, and in neither case were we able to refine the position of the hydride. All the data in Tables I and II refer to the 295 K structure of **3**. In Figure 1 an ORTEP plot of the anion of this salt is given, with the appropriate atomic labeling scheme. The pertinent structural data for the anion are given in Tables I and II, while Table III contains the crystal data and the salient features of the X-ray data collection.

The shortness of the metal–metal separation [W(1)–W(2) = 2.420 (1) Å], the acute angles subtended at the μ-S atoms (~61°), and the values of the various M_2L_9 distortional moduli[16] suggest the presence of strong metal–metal bonding in the anion of **3**. These compare with a W–W distance of 2.41 Å and W–(μ-Cl)–W angles of 58° in the $W_2Cl_9^{3-}$ anion,[17] which is normally considered to contain a W≡W (triple) bond.[18] The W–H bond lengths [W(1)–H(1) = 1.48 Å; W(2)–H(1) = 1.80 Å] are in general

---

(15) Moynihan, K. J. Ph.D. Thesis, University of Calgary, 1983.

(16) Cotton, F. A.; Ucko, D. A. *Inorg. Chim. Acta* **1972**, *6*, 161.

(17) Watson, W. H.; Waser, J. *Acta Crystallogr.* **1958**, *11*, 689.

(18) Summerville, R. H.; Hoffmann, R. *J. Am. Chem. Soc.* **1979**, *101*, 3821.

Table IV. Selected Infrared Data for $Cl_3W(\mu\text{-}H)(\mu\text{-}Me_2S)_2WCl_2(Me_2S)$ (**1**), for Salts of the $[Cl_3W(\mu\text{-}H)(\mu\text{-}Me_2S)_2WCl_3]^-$ Anion, and for Their Deuterio Analogues

complex	ν_{sym}(W–H–W) or ν_{asym}(W–D–W), cm^{-1}	ν_{sym}(W–H–W) or ν_{asym}(W–D–W), cm^{-1}	ν(W–Cl), cm^{-1}
$Cl_3W(\mu\text{-}H)(\mu\text{-}Me_2S)_2WCl_2(Me_2S)$	1637 (mw)	1245 (s)	334 (m), 326 (ms), 314 (vs), 300 (vs), 291 (s), 283 (s)
$Cl_3W(\mu\text{-}D)(\mu\text{-}Me_2S)_2WCl_2(Me_2S)$	1148 (w)	889 (m)	336 (m), 327 (ms), 314 (vs), 299 (vs), 293 (s), 283 (s)
$[Ph_4As][Cl_3W(\mu\text{-}H)(\mu\text{-}Me_2S)_2WCl_3]\cdot{}^1/_2CH_2Cl_2$	1626 (mw)	1234 (ms)	290 (vs), 270 (s)
$[Ph_4As][Cl_3W(\mu\text{-}D)(\mu\text{-}Me_2S)_2WCl_3]\cdot{}^1/_2CH_2Cl_2$	1150 (mw)[a]	900 (m)	294 (vs), 268 (s)
$[Ph_4As][Cl_3W(\mu\text{-}H)(\mu\text{-}Me_2S)_2WCl_3]\cdot{}^1/_2(CH_3)_2CO$	1630 (mw)	1237 (m)	296 (vs), 268 (s)
$[Ph_4As][Cl_3W(\mu\text{-}D)(\mu\text{-}Me_2S)_2WCl_3]\cdot{}^1/_2(CH_3)_2CO$	1157 (w)[a]	893 (m)	295 (vs), 267 (s)
$[Ph_4As][Cl_3W(\mu\text{-}H)(\mu\text{-}Me_2S)_2WCl_3]\cdot{}^1/_2C_2H_4Cl_2$	1634 (mw)	1252 (ms)	300 (vs), 275 (s)
$[Ph_4As][Cl_3W(\mu\text{-}D)(\mu\text{-}Me_2S)_2WCl_3]\cdot{}^1/_2C_2H_4Cl_2$	1158 (w)[a]	896 (m)	302 (vs), 273 (s)
$[Ph_4P][Cl_3W(\mu\text{-}H)(\mu\text{-}Me_2S)_2WCl_3]\cdot 2CH_2Cl_2$	1622 (m)	1223 (ms)	305 (vs), 281 (s)
$[Ph_4P][Cl_3W(\mu\text{-}D)(\mu\text{-}Me_2S)_2WCl_3]\cdot{}^1/_2CH_2Cl_2$	1165 (w)[a]	905 (mw)	301 (vs), 278 (s)
$[Ph_4P][Cl_3W(\mu\text{-}H)(\mu\text{-}Me_2S)_2WCl_3]\cdot{}^2/_3(CH_3)_2CO$	1628 (w)	1234 (m)	305 (vs), 276 (s)
$[Ph_4P][Cl_3W(\mu\text{-}H)(\mu\text{-}Me_2S)_2WCl_3]\cdot{}^3/_4C_2H_4Cl_2$	1632 (m)	1221 (ms)	300 (vs), 277 (s)
$[HPPh_3][Cl_3W(\mu\text{-}H)(\mu\text{-}Me_2S)_2WCl_3]$	1675 (w)	1285 (m)	298 (vs), 273 (s)
$[HPPh_3][Cl_3W(\mu\text{-}D)(\mu\text{-}Me_2S)_2WCl_3]$	1162 (w)[a]	920 (m)[a]	300 (vs), 272 (s)
$[PPN][Cl_3W(\mu\text{-}H)(\mu\text{-}Me_2S)_2WCl_3]\cdot{}^1/_2CH_2Cl_2$	1640 (mw)	*b*	300 (vs), 279 (s)
$[PPN][Cl_3W(\mu\text{-}D)(\mu\text{-}Me_2S)_2WCl_3]\cdot{}^1/_2CH_2Cl_2$	*b*	910 (m)	296 (vs), 274 (s)

[a] Band partially obscured by a cationic band. [b] Band totally obscured by a cationic band.

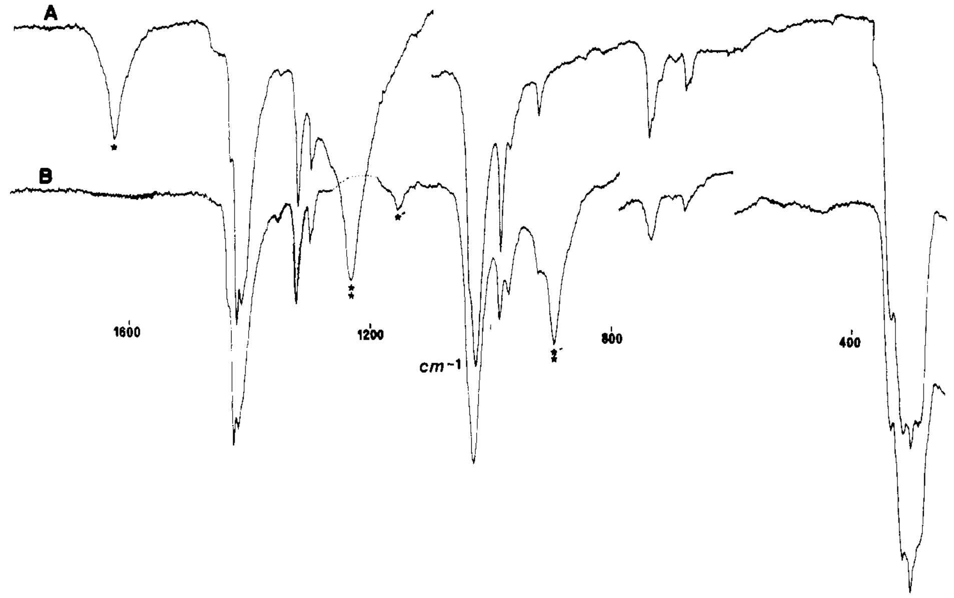

Figure 2. Infrared spectra of the complexes $Cl_3W(\mu\text{-}H)(\mu\text{-}Me_2S)_2WCl_2(Me_2S)$ (A) and $Cl_3W(\mu\text{-}D)(\mu\text{-}Me_2S)_2WCl_2(Me_2S)$ (B). A: (asterisk) ν_{sym}(W–H–W), 1637 cm^{-1}; (two asterisks) ν_{asym}(W–H–W), 1243 cm^{-1}. B: (asterisk) ν_{sym}(W–D–W), 1148 cm^{-1}; (two asterisks) ν_{asym}(W–D–W), 889 cm^{-1}.

agreement with those reported for similar complexes of molybdenum and tungsten (e.g. for $[PyH]_3[Mo_2Cl_8H]$ Mo–H = 1.62 (1), 1.74 (1) Å;[19] for $W_4(\mu\text{-}H)_2(O\textit{i}\text{-}Pr)_{14}$ W–H = 1.61 (8), 1.89 (8) Å.[20]) The well-known structural trans influence of a hydride ligand[21] is demonstrated in the anion of **3**. The W–Cl bond lengths involving the chlorines that are trans to μ-H (Cl(1) and Cl(4)) are significantly longer than the remaining W–Cl bonds in the complex (see Table II). The bridging thioether ligands exhibit relatively short W–S bond lengths (2.372 (5)–2.389 (4) Å), as compared to those found in complexes containing terminal $W\text{–}SR_2$ moieties (e.g. for $(Me_2S)Cl_2W(\mu\text{-}SEt)_3WCl_2(Me_2S)$ $W\text{–}S_t$ = 2.613 (9)–2.623 (4) Å).[22] This feature can now be recognized as a general phenomenon in thioether complexes.[23] Least-squares-planes calculations showed that the anion has approximate C_{2v} symmetry, although this is not crystallographically required.

Infrared Studies. Infrared spectral data for **1**, and for a number of salts of its chloroanionic derivative, are presented in Table IV together with data for analogous deuterio complexes. Bands due to the symmetric and asymmetric W–H–W stretching vibrations of the hydride ligand occur in the regions 1640–1620 cm^{-1} and 1250–1220 cm^{-1}, respectively. The corresponding bands for the deuterio complexes have very similar shapes and are moved to lower frequencies, as expected (ν_{sym} = ~1160–1150 cm^{-1}; ν_{asym} = ~910–895 cm^{-1}). These assignments are based on those of McCarley and Katovic,[24] who examined the infrared spectra of salts of the closely related species $[Cl_3M(\mu\text{-}H)(\mu\text{-}Cl)_2M'Cl_3]^{3-}$ (M = M′ = Mo; M = Mo, M′ = W). The ν(W–Cl) regions of the spectra of salts of the $[Cl_3W(\mu\text{-}H)(\mu\text{-}Me_2S)_2WCl_3]^-$ anion are consistent with the presence of terminal WCl_3 units, having C_{2v} symmetry imposed by the bridging ligands. The data in Table IV indicate that the vibrational spectrum of the $[Cl_3W(\mu\text{-}H)(\mu\text{-}Me_2S)_2WCl_3]^-$ anion is remarkably independent of the cation and of the solvent of crystallization.

The spectrum of the neutral complex, **1** (Figure 2), is notable for the relatively greater intensity of the symmetric ν(W–H–W) stretching mode and for the increased number of bands in the

---

(19) Bino, A.; Cotton, F. A. *J. Am. Chem. Soc.* **1979**, *101*, 332.

(20) Akiyama, M.; Chisholm, M. H.; Cotton, F. A.; Extine, M. W.; Haitko, D. A.; Leonelli, J.; Little, D. *J. Am. Chem. Soc.* **1981**, *103*, 779.

(21) Appleton, T. G.; Clark, H. C.; Manzer, L. E. *Coord. Chem. Rev.* **1973**, *10*, 335.

(22) Boorman, P. M.; Patel, V. D.; Kerr, K. A.; Codding, P. W.; van Roey, P. *Inorg. Chem.* **1980**, *19*, 3508.

(23) Murray, S. G.; Hartley, F. R. *Chem. Rev.* **1981**, *81*, 365.

(24) Katovic, V.; McCarley, R. E. *Inorg. Chem.* **1978**, *17*, 1268.

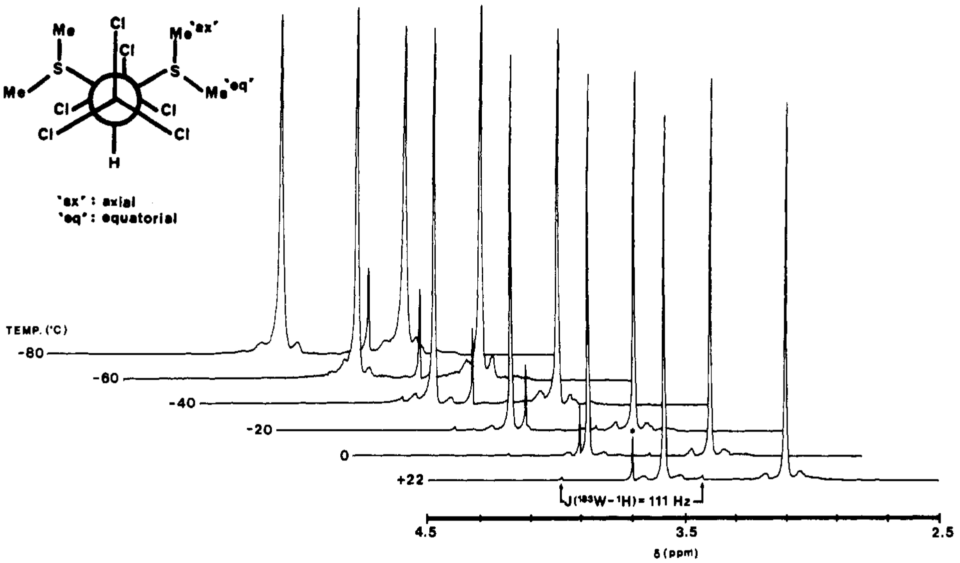

Figure 3. μ-H and μ-Me_2S portions of the 200-MHz ^1H NMR spectra of the complex $[Ph_4P][Cl_3W(\mu\text{-}H)(\mu\text{-}Me_2S)_2WCl_3]\cdot 2CH_2Cl_2$ (3) recorded between -80 and +22 °C in CD_2Cl_2 solvent.

ν(W–Cl) region (which would be expected for a compound of lower symmetry). As noted below, this compound exists as a mixture of isomers, which would add to the complexity of the IR spectrum. The deuterio analogue of **1** has an identical spectrum, with the exception of the bands assigned to ν(W–D–W) modes. These are shifted to lower wavenumber as described for the chloroanionic species above.

NMR Studies. The ^1H NMR spectra of salts of the $[Cl_3W(\mu\text{-}H)(\mu\text{-}Me_2S)_2WCl_3]^-$ anion may be interpreted on the basis of the Newman-type projection of this species, as shown in the inset diagram of Figure 3. Two sets of magnetically equivalent protons should exist for the axial and equatorial methyl groups of the μ-Me_2S ligands. Thus the methyl region of its spectrum should consist of two singlets of equal intensity. The hydride resonance, of intensity 1:6 with respect to each of the methyl resonances, might be expected to display coupling to ^{183}W (^{183}W, $I = {}^1/_2$, 14.4% natural abundance). Spectra of the anion were recorded for a variety of counterions (Ph_4P^+; Ph_4As^+, PPN^+, Ph_3PH^+) and found to be independent of the nature of the cation (Experimental Section). The set of temperature-dependent spectra displayed in Figure 3 illustrates the features expected and one that was quite unexpected. The spectra were recorded for the compound $[Ph_4P][Cl_3W(\mu\text{-}H)(\mu\text{-}Me_2S)_2WCl_3]\cdot 2CH_2Cl_2$ over the range -80 to +22 °C in CD_2Cl_2 solution. The 22 °C spectrum contains two singlets at δ 3.10 and 3.58 for the Me groups, of intensity 6, and a resonance of intensity 1 at δ 3.71, flanked by two satellites. The ^1H NMR spectra of salts of the analogous μ-deuterio anion, $[Cl_3W(\mu\text{-}D)(\mu\text{-}Me_2S)_2WCl_3]^-$, are devoid of this resonance, but the ^2H spectra, measured in CH_2Cl_2 solution, possess a resonance at δ ~3.5–3.7 with $J(^{183}W\text{-}^2H)$ ~ 17 Hz. Thus the chemical shift of the μ-H ligand of the $[Cl_3W(\mu\text{-}H)(\mu\text{-}Me_2S)_2WCl_3]^-$ anion occurs at a relatively low-field position.[25] Several other examples of hydride resonances appearing downfield from Me_4Si have been reported recently.[20,26,27] For example, Chisholm, Cotton, and co-workers[20] reported that for $W_4(\mu\text{-}H)_2(O\textit{i}\text{-}Pr)_{14}$ the hydride resonance appears as a singlet at δ 7.87, with $J(^{183}W\text{-}^1H) = 96$ Hz. The unusual feature of the spectra shown in Figure 3 is the temperature dependence of the μ-H chemical shift. Whereas the methyl resonances are insensitive to temperature change, the hydride resonance moves in a linear fashion to higher field as the temperature is lowered. Coupling to ^{183}W remains constant over this range, with $J(^{183}W\text{-}^1H) = 111 \pm 3$ Hz, suggesting that the W–H–W linkage remains intact in solution between -80 and +22 °C. We ascribe this temperature dependence to the proximity of the hydride ligand to the metal–metal bonding electron density, which might be expected to be delicately sensitive to slight population adjustments over the ~100 °C temperature range studied. Clearly any such effect could result in a change in the anisotropic magnetic field at the hydride location.

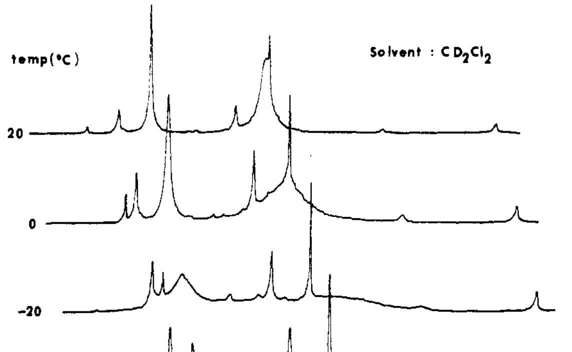

Figure 4. Temperature dependence of the ^1H NMR spectrum of $Cl_3W(\mu\text{-}H)(\mu\text{-}Me_2S)_2WCl_2(Me_2S)$ measured at 200 MHz in CD_2Cl_2 from -70 to +20 °C.

The ^1H NMR spectrum of the neutral compound, **1**, exhibits a number of unexpected features that are worthy of comment. The spectra recorded between -70 °C and +20 °C in CD_2Cl_2 solution are shown in Figure 4. From the low-temperature spectrum it can be deduced that two different geometric isomers are present in solution. These are depicted in Figure 5. The meso compound (C_s symmetry) would be expected to exhibit a ^1H NMR spectrum consisting of three singlets, intensity 6:6:6, for methyl

---

[25] Moore, D. S.; Robinson, S. D. *Chem. Soc. Rev.* **1983**, *12*, 415.
[26] (a) Wilson, R. B.; Sattelberger, A. P.; Huffman, J. C. *J. Am. Chem. Soc.* **1982**, *104*, 858. (b) Sattelberger, A. P.; Wilson, R. B.; Huffman, J. C. *Inorg. Chem.* **1982**, *21*, 479.
[27] Belmonte, P. A.; Schrock, R. R.; Day, C. S. *J. Am. Chem. Soc.* **1982**, *104*, 3082.
[28] Grynkewich, G. W.; Marks, T. J. *Inorg. Chem.* **1976**, *15*, 1307.

Table V. Assignments for the −70 and +20 °C ^1H NMR Spectra of $Cl_3W(\mu\text{-}H)(\mu\text{-}Me_2S)_2WCl_2(Me_2S)$ in CD_2Cl_2 Solution (see Figure 4)[a]

−70 °C spectrum			+20 °C spectrum		
resonance position, ppm	rel intens	assgnt	resonance position, ppm	rel intens	assgnt
3.77	s	equatorial Me groups of *dl*	3.76	m	μ-H of *dl*
3.69	s		3.62	m	equatorial Me groups of meso
3.63	m	equatorial Me groups of meso			
			3.49	ms	bridging Me_2S of *dl*, not involved in site exchange
3.31	m	μ-H of *dl*			
3.24	s	axial Me groups of *dl*			
3.13	s		3.36	w	μ-H of meso
3.16	ms	axial Me groups of meso	3.15	m	axial Me groups of meso
2.96	m	terminal Me_2S of meso	3.03	s	fluxional Me_2S of *dl*
2.78	s	terminal Me_2S of *dl*	3.01	m	terminal Me_2S of meso
2.35	s				
2.08	w	free Me_2S			

[a] Abbreviations: *dl*, enantiomeric pair of C_1 symmetry; meso, isomer with C_s symmetry s, strong; m, medium, w, weak. The absolute assignment of ^1H resonances to equatorial or axial protons on the μ-Me_2S ligands is tentative and based on the earlier assignments of Boorman and Patel,[14] and of Grynkewich and Marks[28] for $(\mu\text{-}PhMeSn)_2Fe_2(CO)_7$ isomers.

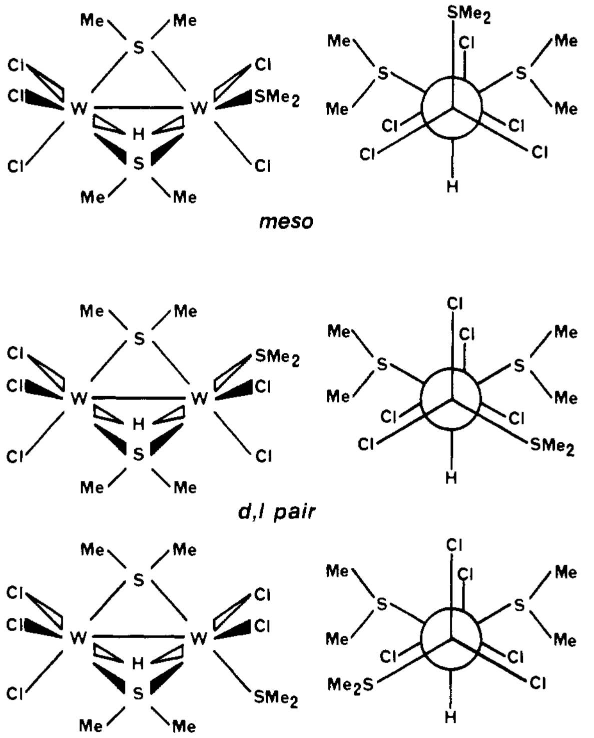

Figure 5. Possible geometric isomers for the complex $Cl_3W(\mu\text{-}H)(\mu\text{-}Me_2S)_2WCl_2(Me_2S)$ (**1**).

protons in axial, equatorial (both bridging), and terminal positions and a hydride signal. This spectrum would be unaffected by temperature. However the C_1 isomer (for which a pair of enantiomers exists) would exhibit separate signals for each methyl group in the low-temperature limit, since in the absence of inversion at sulfur, even the terminal Me_2S methyl groups would be nonequivalent. Hence, in addition to a hydride signal, six singlets should appear in the low-temperature spectrum of which two would be in the "axial", two in the "equatorial", and two in the terminal Me_2S methyl group region of the spectrum. Assignments for the low-temperature and high-temperature limiting spectra are given in Table V. It can be seen that the low-temperature spectrum is consistent with the predictions above. The ratio of the isomer concentrations is approximately 4:1 C_1:C_s. However, if isolated from the reaction flask after longer periods of stirring, the product was found to contain an increasing proportion of the C_s isomer. The resonances due to μ-H ligands occur at δ 3.8 for the C_1 enantiomers and at δ 3.04 for the C_s (meso) isomer. Expansion of the spectra enables an assignment of the ^{183}W satellites for the C_1 isomers, with $J(^{183}W\text{-}^1H) = 109$ Hz. The resonance due to μ-H in the C_s isomer is insufficiently intense to assign satellites, but both isomers exhibit movement of the μ-H resonance downfield as the temperature is increased. This behavior is very similar to that described above for the anion of **3**. Confirmation of these assignments was obtained from spectral studies of the ^2H-substituted compound, both by observation of the ^2H spectra and by the absence of the relevant resonances in the ^1H spectra of these derivatives.

If the spectra (Figure 4) are followed as the temperature is increased from −70 °C, it can be seen that at least two fluxional processes occur, and both of these are identified as belonging to the pair of C_1 enantiomers. The two resonances for the terminal Me_2S protons in the C_1 isomers collapse into a singlet upon increase in temperature, as a fluxional process (usually described as inversion at S)[29] allows the methyl groups to become magnetically equivalent. This is accompanied by a second fluxional process, which involves the site exchange between the terminal Me_2S ligand and the bridging Me_2S ligand trans to it. In the high-temperature limit, as shown in the 20 °C spectrum, only two methyl resonances occur for the C_1 enantiomers; one corresponds to the two Me_2S ligands involved in the exchange process, and this occurs at a δ value intermediate between the terminal and bridging regions, and the other (of half the intensity) occurs at an average position between the original (low-temperature) axial and equatorial resonances for the C_1 isomer. This is assigned to a nonexchanging μ-Me_2S ligand, whose two sets of protons are rendered equivalent by the fluxional process.

This process, which is depicted in the sequence below (Scheme II), interconverts the two enantiomers and clearly affords a unique opportunity to observe a racemization process for a pair of confacial bioctahedral isomers. The question arises, however, as to why only the *dl* pair is fluxional and the meso isomer is inert at temperatures between −70 and +20 °C. As shown in Scheme II, it must be the pair of trans Me_2S groups that is exchanging between bridging and terminal sites. This requires, as the first step, the breaking of the bond (c) indicated in the diagram

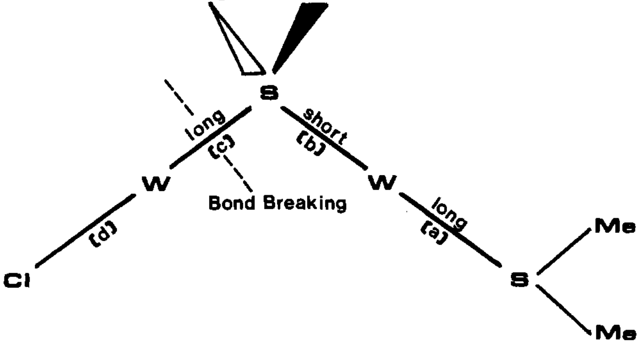

---

(29) Abel, E. W.; Bhatti, M. M.; Orell, K. G.; Sik, V. *J. Organomet. Chem.* **1981**, *208*, 195.

Scheme II

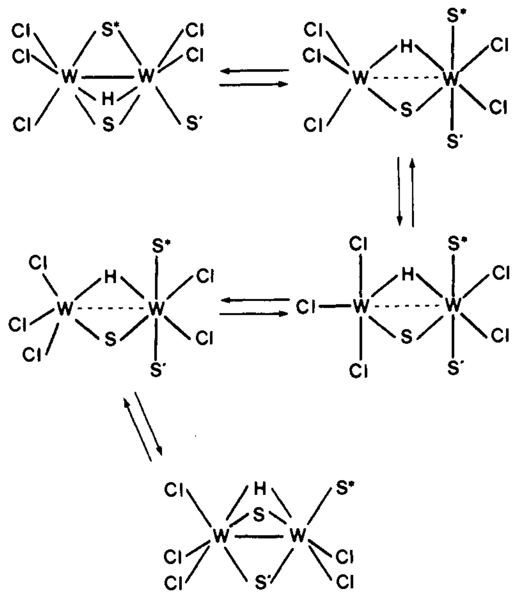

$S \equiv SMe_2$

Although structural data are not available for complex **1**, we have recently determined the structures of two similar complexes, in which a terminal Me_2S ligand forms a long M–S bond (a) trans to a relatively short bond to the bridging ligand (b).[30,31] The next bond (c) is significantly longer and is trans to a chloride ligand in both structures. This, we believe, is responsible for the easy cleavage of bond c and creates a simple mechanism for racemization. During this process the WCl_3 unit on W(2) would undergo inversion, relative to the W–W vector, as shown in Scheme II. Since this involves a five-coordinate metal atom in the intermediate, the process is essentially a Berry pseudorotation, although in this instance the trigonal-bipyramidal structure is intermediate between two square-pyramidal moieties, rather than vice versa.

The possibility of the site exchange occurring by a process involving dissociation of the terminal Me_2S was considered, but since the spectra are unchanged by the addition of a large excess of Me_2S, at both −70 and +20 °C, we strongly favor the intramolecular process proposed above.

Although the major fluxional processes are identified in the foregoing discussion, the presence of a weak resonance due to free Me_2S, which undergoes broadening as the temperature is increased, suggests that, in addition to the above processes, exchange of free and coordinated Me_2S may be occurring. The species so produced might explain some of the weak unassigned lines in the ^1H NMR spectra at certain temperatures. It must be stressed, however, that this is a minor component of the reaction system, unless the temperature is raised to above 40 °C.

Conclusions

Although the original intent of this work was to identify reactions of hydride with organosulfur ligands in the coordination sphere of tungsten, the major achievement was the isolation and characterization of a series of novel bis(thioether)-bridged ditungsten(III) complexes. The bridging moiety, $[(\mu\text{-H})(\mu\text{-Me}_2S)_2]$, has not been reported before for any binuclear transition-metal complexes. From the criteria of Summerville and Hoffmann,[18] this set of bridging ligands would be expected to favor strong metal–metal interaction between two d^3 centers. This is consistent with the observed short $W\equiv W$ distance, 2.419 (1) Å, in the anion of **3**. The other unusual feature of these complexes is the temperature dependence of the chemical shift for the μ-H entity, which was discussed in detail above.

The neutral complex of $Cl_3W(\mu\text{-H})(\mu\text{-Me}_2S)_2WCl_2(Me_2S)$ (**1**) was shown by ^1H NMR to exist as a mixture of two isomers, viz. a meso isomer of C_s symmetry and a *dl* pair of enantiomers (C_1 symmetry). A stereospecific exchange of terminal and bridging Me_2S ligands enables the interconversion of the *dl* pair, while the meso isomer does not exhibit any fluxionality. This exchange process also causes the axial and equatorial methyl groups of the nonexchanging $\mu\text{-Me}_2S$ ligand to be equivalent. The process described here is very similar to that suggested by Grynkewich and Marks[28] for the interchange of terminal and bridging CO groups in the complexes $(CO)_3Fe(\mu\text{-SnR}_2)_2(\mu\text{-CO})_3$. The simultaneous occurrence of a second fluxional process in our system, namely the process that makes the two sets of protons equivalent on the terminal Me_2S ligand in the C_1 isomers, prohibits the application of simple procedures to obtain a free energy of activation for the racemization process in the case of **1**.

Experimental Section

General Procedures. The adduct $WCl_4(Me_2S)_2$ was prepared by direct reaction of WCl_4 and the ligand as described previously.[32] Tungsten hexachloride (Alfa) was twice sublimed at ~225 °C in flame-sealed evacuated Pyrex glass tubes prior to use in order to remove oxychloride impurities. Triethylsilane and chlorotrimethylsilane (Petrarch) were used as received, but all solvents were dried and degassed by standard methods. All handling of starting materials, reaction solutions, and products was done in an atmosphere of pure, dry nitrogen. The salts tetraphenylphosphonium chloride and bis(triphenylphosphine)nitrogen(1+) chloride were obtained from Alfa and used as received; tetraphenylarsonium chloride (Alfa) was dried at ~120 °C under vacuum for ~24 h. The deuterated solvents $CDCl_3$, CD_2Cl_2, and $C_2D_2Cl_4$ (Merck, Sharp and Dohme) were used as received. Triethylsilane-d_1, (Et_3SiD), was prepared by the reaction of Et_3SiCl with $LiAlD_4$ in Et_2O. The compounds $Me_3Si(SR)$ (R = Me, Et, Ph) were synthesized by reacting excess Me_3SiCl with the lead salts $[Pb(SR)_2]_n$ (R = Me, Et, Ph) of the parent thiols according to the published procedure.[33] Elemental analyses were obtained commercially (Galbraith Laboratories Inc., Knoxville, TN) or were undertaken in our laboratories as described previously.[32]

Gas chromatographic analyses were performed on a Varian 3700 GC, equipped with a Porapak Q column and a thermal conductivity detector. For GC–MS analysis a Hewlett-Packard 5840A GC, interfaced to a Micromass 7070F mass spectrometer, was used. Infrared spectra (4000–250 cm^{-1}; Nujol mulls between CsI plates or KBr disks) were run by using either a Perkin-Elmer 467 or 580 dispersive instrument. For higher resolution far-IR spectra, a Nicolet 8000 FTIR spectrometer was used, with the sample contained as a Nujol mull between polyethylene windows. UV–visible absorption spectra in the range 250–850 nm were obtained at room temperature on a Varian-Cary 219 spectrophotometer and 10-mm matched quartz cells.

Routine room-temperature ^1H NMR spectra were recorded at 60 MHz with a Hitachi Perkin Elmer R-24B spectrometer. All other ^1H NMR spectra were measured at 200 MHz on a Varian XL-200 FT spectrometer, with a deuterium lock. Variable-temperature spectra were also recorded on this system in the range −80 to +40 °C, as the solvent properties and compound stability permitted. Chemical shifts are reported on the δ scale in ppm relative to Me_4Si. ^2H NMR spectra were run in CH_2Cl_2 solution at 23 °C and were recorded at 30.71 MHz on the XL-200 instrument. The ^2H signal was referenced to $CHDCl_2$ in the solvent (5.31 ppm downfield from the ^2H resonance of $Me_4Si\text{-}d_{12}$).

Synthesis and Characterization of the New Compounds. $[WCl_3(SR)]_n$ **(R = Me, Et, Ph).** Only the synthesis of $[WCl_3(SMe)]_n$ will be described since the procedures for the ethyl and phenyl analogues are entirely equivalent. To a stirring solution of WCl_6 (1.50 g, 3.8 mmol) in CH_2Cl_2 (~150 mL) the exact 1 molar equiv of $Me_3Si(SMe)$ was added, also in CH_2Cl_2 solution. After the mixture was stirred for 15 min to ensure that the metathesis had occurred, 1 molar equiv of Et_3SiH was added, dissolved in ~10 mL of CH_2Cl_2. A rust-colored precipitate formed immediately, and gas evolution was observed from the solution. After ~1 h the solution was filtered, and the solid was washed, on the frit, with CH_2Cl_2 (3 × 5 mL) and hexane (3 × 5 mL). After drying in vacuo at 70 °C for 5 h, the product was weighed and analyzed. Yield: 0.91 g, 71%. Anal. Calcd for $[WCl_3(SCH_3)]$: W, 54.51; Cl, 31.53; S, 9.51; C,

---

[30] Boorman, P. M.; Ball, J. M.; Moynihan, K. J.; Patel, V. D.; Richardson, J. F. *Can. J. Chem.* **1983**, *61*, 2809.

[31] Boorman, P. M.; Moynihan, K. J.; Oakley, R. T. *J. Chem. Soc., Chem. Commun.* **1982**, 899.

[32] Boorman, P. M.; Chivers, T.; Mahadev, K. N. *Can. J. Chem.* **1975**, *53*, 383.

[33] Abel, E. W. *J. Chem. Soc.* **1960**, 4406.

3.56; H, 0.90. Found: W, 53.1; Cl, 31.6; S, 9.61; C, 3.71; H, 1.06. IR data (2000–250 cm^{-1}, Nujol mull, CsI plates): 1409 (mw), 1402 (mw), 1290 (ms), 1036 (vw), 999 (w), 983 (w), 951 (m), 379 (vs), 357 (s) [340 (sh)], 302 (mw) [307 (sh), 296 (sh)], 286 (w) cm^{-1}.

$[WCl_3(SEt)]_n$: Anal. Calcd for $[WCl_3(SC_2H_5)]$: W, 52.33; Cl, 30.27. Found: W, 53.2; Cl, 29.8. IR data: 1588 (mw), 1416 (m), 1250 (s), 1052 (mw), 1032 (w), 996 (m), 968 (ms), 764 (m), 614 (w), 478 (w), 421 (mw), 374 (vs), 350 (s).

$[WCl_3(SPh)]_n$: Anal. Calcd for $[WCl_3(SC_6H_5)]$: W, 46.04; Cl, 26.63. Found: W, 47.8; Cl, 27.0. IR data: 1576 (m), 1277 (vw), 1185 (mw), 1163 (mw), 1023 (m), 1001 (s), 742 (vs), 686 (ms), 479 (mw), 380 (vs), 352 (s), 308 (w).

These compounds are all very air sensitive and insoluble in common organic solvents.

Preparation of $Cl_3W(\mu\text{-}H)(\mu\text{-}Me_2S)_2WCl_2(Me_2S)$ (1). To a stirred solution of $WCl_4(Me_2S)_2$ (4.64 g, 10.3 mmol) in CH_2Cl_2 (~60 mL) was added neat Et_3SiH (4.79 g, 41.2 mmol). The solution, originally clear and orange-red, darkened in color, and after it was stirred for ~5 h, a purple solid began to precipitate. This precipitation continued, and after ~20 h, the solution was filtered. The purple solid that remained on the frit was washed with CH_2Cl_2 (2 × 2 mL) and dried in vacuo at 50 °C for 3 h. Yield: 2.1 g (56%, based on $WCl_4(Me_2S)_2$). The compound was found to be nonconducting in CH_2Cl_2 solution and diamagnetic and in spite of numerous attempts, failed to produce X-ray quality crystals. The solid can be handled for brief periods in air without decomposition, but solutions are susceptible to reaction with moisture. Both the solid and its solution are unstable above ~50 °C. It was formulated as $Cl_3W(\mu\text{-}H)(\mu\text{-}Me_2S)_2WCl_2(Me_2S)$. Anal. Calcd for $W_2Cl_5S_3C_6H_{19}$: W, 50.21; Cl, 24.20; S, 13.13; C, 9.84; H, 2.62. Found: W, 48.4; Cl, 23.4; S, 12.3; C, 9.79; H, 2.68. IR data (KBr disk): see Table IV. UV–visible absorption spectral data (CH_2Cl_2 solution, nm, with ϵ in parentheses): 562 (1800), 368 (7400), 321 (5500).

Synthesis of $Cl_3W(\mu\text{-}D)(\mu\text{-}Me_2S)_2WCl_2(Me_2S)$. The procedure used was the same as that described for **1** above, but in place of Et_3SiH, Et_3SiD was used. IR spectrum: see Table IV.

Preparation of $[Ph_3PH][Cl_3W(\mu\text{-}H)(\mu\text{-}Me_2S)_2WCl_3]$ (2). The complex was prepared serendipitously, as follows: **1** (0.52 g, 0.7 mmol) was dissolved in CH_2Cl_2 (~150 mL), and Ph_3P (0.18 g, 0.7 mmol), dissolved in CH_2Cl_2 (5 mL), was added. The solution became purple-red, and after being stirred for 10 h at 22 °C, it was filtered to yield a clear solution, which was evaporated to dryness under vacuum. The purple-red glassy solid so produced was recrystallized from $CHCl_3$/hexane to give purple-red crystals of $[HPPh_3][Cl_3W(\mu\text{-}H)(\mu\text{-}Me_2S)_2WCl_3]$. Yield: 0.3 g, 44%. IR (Table IV) and NMR data were discussed in the text.

The deuterio-bridged complex **$[Ph_3PH][Cl_3W(\mu\text{-}D)(\mu\text{-}Me_2S)_2WCl_3]$** was prepared entirely analogously, from $Cl_3W(\mu\text{-}D)(\mu\text{-}Me_2S)_2WCl_2(Me_2S)$ and Ph_3P in CH_2Cl_2.

Syntheses of Complexes of the Type $[Q][Cl_3W(\mu\text{-}X)(\mu\text{-}Me_2S)_2WCl_3]\cdot n$(solvent) (X = H, D; Q = PPN^+, Ph_4As^+, Ph_4P^+; solvent = CH_2Cl_2, $(CH_3)_2CO$, $C_2H_4Cl_2$; $n = {}^1/_2$–2). These syntheses all followed the same basic pattern, and only one is described here. **$[Ph_4P][Cl_3W(\mu\text{-}H)(\mu\text{-}Me_2S)_2WCl_3]\cdot 2CH_2Cl_2$** was prepared by dissolving $Cl_3W(\mu\text{-}H)(\mu\text{-}Me_2S)_2WCl_2(Me_2S)$ (0.70 g, 0.95 mmol) in CH_2Cl_2 (~100 mL) and adding $[Ph_4P]Cl$ (0.36 g, 0.95 mmol). The solution was stirred at 22 °C for 10 h and then filtered and evaporated to dryness. The red-purple glassy solid so produced was redissolved in CH_2Cl_2 (~15 mL), and to this clear purple-red solution was added hexane (~5 mL). Cooling to −20 °C for 48 h yielded purple-red crystals of **3**. Yield: 0.82 g, 71%. Complete characterization of **3** by X-ray methods is described above. Other members of this class were identified by comparison of their spectroscopic properties with those of **3**, and also of **2**, whose structure was reported earlier.[11] IR data are presented in Table IV. Other spectroscopic data are as follows:

(a) ^1H NMR Data (at Room Temperature Unless Otherwise Stated). $[PPN][Cl_3W(\mu\text{-}H)(\mu\text{-}Me_2S)_2WCl_3]\cdot{}^1/_2CH_2Cl_2$ (in $C_2D_2Cl_4$): 7.62–7.33 [m, 30 H, $[(Ph_3P)_2N]^+$], 5.28 [s, 1 H, CH_2Cl_2 (of crystallization)], 3.82 (22 °C) [s, 1 H, μ-H, $J(^{183}W\text{–}^1H)$ = 108 Hz], 3.63 [s, 6 H, μ-Me_2S (equatorial)], 3.09, [s, 6 H, μ-Me_2S (axial)].

$[Ph_4As][Cl_3W(\mu\text{-}H)(\mu\text{-}Me_2S)_2WCl_3]\cdot{}^1/_2CH_2Cl_2$ (in $C_2D_2Cl_4$): 7.83–7.47 [m, 20 H, $[Ph_4As]^+$], 5.25 [s, 1 H, CH_2Cl_2 (of crystallization)], 3.79 (22 °C) (3.50 at −40 °C) [s, 1 H, μ-H, $J(^{183}W\text{–}^1H)$ = 109 Hz], 3.57 [s, 6H, μ-Me_2S (equatorial)], 3.06 [s, 6 H, μ-Me_2S (axial)].

$[Ph_4As][Cl_3W(\mu\text{-}H)(\mu\text{-}Me_2S)_2WCl_3]\cdot{}^1/_2(CH_3)_2CO$ (in $C_2D_2Cl_4$): 7.85–7.45 [m, 20 H, $[Ph_4As]^+$], 3.80 (21 °C) [s, 1 H, μ-H, $J(^{183}W\text{–}^1H)$ = 110 Hz], 3.58 [s, 6 H, μ-Me_2S (equatorial)], 3.07 [s, 6 H, μ-Me_2S (axial)], 2.10 [s, 3 H, $(CH_3)_2CO$ (of crystallization)].

$[Ph_4As][Cl_3W(\mu\text{-}H)(\mu\text{-}Me_2S)_2WCl_3]\cdot{}^1/_2C_2H_4Cl_2$ (in CD_2Cl_2): 7.89–7.57 [m, 20 H, $[Ph_4As]^+$], 3.75 [s, 2 H, $C_2H_4Cl_2$ (of crystallization)], 3.71 (23 °C) [s, 1 H, μ-H, $J(^{183}W\text{–}^1H)$ = 110 Hz], 3.59 [s, 6 H, μ-Me_2S (equatorial)], 3.11 [s, 6 H, μ-Me_2S (axial)].

$[Ph_4P][Cl_3W(\mu\text{-}H)(\mu\text{-}Me_2S)_2WCl_3]\cdot 2CH_2Cl_2$ (in $C_2D_2Cl_4$): 7.87–7.43 [m, 20 H, $[Ph_4P]^+$], 5.25 [s, 4 H, CH_2Cl_2 (of crystallization)], 3.77 (22 °C) [s, 1 H, μ-H, $J(^{183}W\text{–}^1H)$ = 110 Hz], 3.55 [s, 6 H, μ-Me_2S (equatorial)], 3.04 [s, 6 H, μ-Me_2S (axial)].

$[Ph_4P][Cl_3W(\mu\text{-}H)(\mu\text{-}Me_2S)_2WCl_3]\cdot{}^2/_3(CH_3)_2CO$ (in CD_2Cl_2): 7.92–7.55 [m, 20 H, $[Ph_4P]^+$], 3.72 (22 °C) [s, 1 H, μ-H, $J(^{183}W\text{–}^1H)$ = 108 Hz], 3.60 [s, 6 H, μ-Me_2S (equatorial)], 3.11 [s, 6 H, μ-Me_2S (axial)], 2.11 [s, 4 H, $(CH_3)_2CO$ (of crystallization)].

$[Ph_4P][Cl_3W(\mu\text{-}H)(\mu\text{-}Me_2S)_2WCl_3]\cdot{}^3/_4C_2H_4Cl_2$ (in CD_2Cl_2): 7.91–7.57 [m, 20 H, $[Ph_4P]^+$], 3.75 [s, 3 H, $C_2H_4Cl_2$ (of crystallization)], 3.73 (22 °C) [s, 1 H, μ-H, $J(^{183}W\text{–}^1H)$ = 108 Hz], 3.58 [s, 6 H, μ-Me_2S (equatorial)], 3.11 [s, 6 H, μ-Me_2S (axial)].

$[Ph_3PH][Cl_3W(\mu\text{-}H)(\mu\text{-}Me_2S)_2WCl_3]$ (in CD_2Cl_2): 7.83–7.69 [m, 15 H, $[Ph_3PH]^+$], 3.60 [s, 7 H, μ-Me_2S (equatorial) + μ-H (22 °C), $J(^{183}W\text{–}^1H)$ = 109 Hz] [$\delta(\mu\text{-}H)$ 3.24 at −80 °C], 3.14 [s, 6 H, μ-Me_2S (axial)]. The acidic proton of the $[Ph_3PH]^+$ cation was not observed in the spectrum. (^{31}P NMR data (Varian XL-200 spectrometer operating at 80.98 MHz; external 85% H_3PO_4 as a reference; CD_2Cl_2 solution; 23 °C): δ 4.32 [$J(^{31}P\text{–}^1H)$ = 535 Hz], $[Ph_3PH]^+$].)

(b) UV–Visible Spectra (Measured in CH_2Cl_2 Solution, 22 °C). Values are quoted in nm with ϵ (M^{-1} cm^{-1}) in parentheses.

$[Ph_4P][Cl_3W(\mu\text{-}H)(\mu\text{-}Me_2S)_2WCl_3]\cdot 2CH_2Cl_2$: 550 (1300), [480 (sh) (530)], 369 (6000), 316 (4200).

$[Ph_4As][Cl_3W(\mu\text{-}H)(\mu\text{-}Me_2S)_2WCl_3]\cdot{}^1/_2CH_2Cl_2$: 550 (1300), [478 (sh) (510)], 367 (6300), 315 (4500).

$[PPN][Cl_3W(\mu\text{-}H)(\mu\text{-}Me_2S)_2WCl_3]\cdot{}^1/_2CH_2Cl_2$: 550 (1400), [480 (sh) (560)], 368 (6600), 314 (4700).

These salts can all be handled for brief periods in air, but solutions are moisture and thermally sensitive.

X-ray Analysis. A burgundy-colored crystal with approximate dimensions of 0.09 × 0.23 × 0.25 mm^3, which had been coated with epoxy to minimize decomposition, was mounted in an arbitrary orientation on an Enraf-Nonius CAD4F automated diffractometer and optically centered. The cell was identified as triclinic by using the indexing routines of the instrument. The space group $P\bar{1}$ was chosen on the basis of the centric distribution of E values,[34] and the successful solution of the structure supported this selection. Intensity data were measured by using the ω–2θ technique and were corrected for background, Lorentz, and polarization effects. Three standard reflections measured every 1500 s of X-ray exposure time showed that no decomposition had occurred during the data acquisition period. An absorption correction was applied by using the Gaussian method[35] with a 10 × 10 × 12 grid. The crystal data and experimental conditions are summarized in Table III.

The positions of the W atoms were obtained from a three-dimensional Patterson synthesis. Structure factor and difference Fourier calculations revealed the positions of the remaining non-hydrogen atoms. The structure was refined by full-matrix least-squares techniques based on F, minimizing the function $\sum w(|F_o| - |F_c|)^2$, where w was defined as $[\sigma^2(F_o)]^{-1}$, in the final cycles. Scattering factors used for non-hydrogen atoms were those of Cromer and Mann,[36] and anomalous dispersion corrections were included for all non-hydrogen atoms.[37] All hydrogen atoms were located in a difference Fourier synthesis and included in idealized positions (sp^2, C–H = 0.95 Å; sp^3, C–H = 1.00 Å) but were not refined. H atoms were assigned isotropic thermal parameters 1.1 times that of the atom to which they are bonded. The hydride atom was found in a difference Fourier synthesis with an electron density of 0.8 e $Å^{-3}$. As a check on the appropriateness of this assignment, a series of ΔF maps were calculated for various $(\sin\theta)/\lambda$ limits in the data.[38] The maps were all found to have areas of positive electron density in the region of the proposed hydride. The hydride (H(1)) could not be refined and was therefore included with an isotropic (U) thermal parameter of 0.05 $Å^2$.

In the final cycles the W, S, P, Cl, and non-phenyl C atoms were refined anisotropically, the phenyl C atoms were refined isotropically, and the H atoms were redetermined. An isotropic extinction parameter could not be refined successfully. The highest peak in a final difference Fourier is approximately 2.7 e $Å^{-3}$ and is associated with the W atoms. Final atomic positional parameters for the non-hydrogen atoms of the anion are presented in Table I. The remaining non-hydrogen positional pa-

---

(34) All computations were performed with the XRAY-76 system of programs implemented on a Honeywell computer with a Multics operating system. Stewart, J. M., Ed. Technical Report TR-446; Computer Science Center, University of Maryland: College Park, MD, 1976.

(35) CADABS, a local modification of a program by: Coppens, P. *Acta Crystallogr.* **1965**, *18*, 1035.

(36) Cromer, D. T.; Mann, T. B. *Acta Crystallogr. Sect. A: Cryst. Phys., Diffr., Theor. Gen. Crystallogr.* **1968**, *A24*, 321.

(37) "International Tables of X-Ray Crystallography"; Kynoch Press: Birmingham, England, 1974.

(38) La Placa, S. J.; Ibers, J. A. *Acta Crystallogr.* **1965**, *18*, 511.

Inorg. Chem. **1985**, *24*, 2997–3002 **2997**

rameters, thermal parameters, H atom parameters, and the table of observed and calculated structure amplitudes have been deposited.

Acknowledgment. We thank the Natural Sciences and Engineering Research Council of Canada for financial support (to P.M.B. and K.J.M.) and Dr. K. Ann Kerr for the use of the diffractometer. The experimental assistance of J. M. Ball, C. L. Merritt, and Dr. S. Nandana and Dr. R. Yamdagni's advice and help in obtaining spectroscopic data are gratefully acknowledged. We also thank Dr. Scott Collins for helpful discussions.

Registry No. *meso*-**1**, 97371-16-9; *dl*-**1** (isomer I), 97371-17-0; **2**, 81609-97-4; **3**, 97295-68-6; $[WCl_3(SMe)]$, 97295-72-2; $[WCl_3(SEt)]$, 97295-74-4; $[WCl_3(SPh)]$, 97295-76-6; $Me_3Si(SMe)$, 3908-55-2; $Me_3Si(SEt)$, 5573-62-6; $Me_3Si(SPh)$, 4551-15-9; WCl_6, 13283-01-7; $WCl_4(Me_2S)_2$, 53922-82-0; Et_3SiH, 617-86-7; $[PPN][Cl_3W(\mu\text{-}H)(\mu\text{-}Me_2S)_2WCl_3]$, 97295-69-7; $[Ph_4As][Cl_3W(\mu\text{-}H)(\mu\text{-}Me_2S)_2WCl_3]$, 97295-70-0; D_2, 7782-39-0; W, 7440-33-7.

Supplementary Material Available: Tables containing positional parameters for the non-hydrogen atoms of the cation and solvate molecules in complex **3** (Table SI), thermal parameters for all non-hydrogen atoms for complex **3** (Table SII), positional and isotropic thermal parameters for the hydrogen atoms of complex **3** (Table SIII), and bond distances (Table SIV) and bond angles (Table SV) for the Ph_4P^+ cation and CH_2Cl_2 solvate molecules of complex **3**, a view of the unit cell contents of $[Ph_4P][Cl_3W(\mu\text{-}H)(\mu\text{-}Me_2S)_2WCl_3]\cdot 2CH_2Cl_2$ (**3**) (Figure S1), and a listing of the observed and calculated structure factors and $\sigma(F)$ values for complex **3** (33 pages). Ordering information is given on any current masthead page.

Contribution from Research and Development, Phillips Petroleum Company, Bartlesville, Oklahoma 74004,
and the Department of Chemistry, Indiana University, Bloomington, Indiana 47405

Bimetallic Halides. Crystal Structure of and Ethylene Polymerization by $VCl_2\cdot ZnCl_2\cdot 4THF$

PAUL D. SMITH,[†] JOEL L. MARTIN,*[†] JOHN C. HUFFMAN,[‡] RICK L. BANSEMER,[‡]
and KENNETH G. CAULTON*[‡]

Received November 27, 1984

The title compound is prepared either by the zinc reduction of $VCl_4(THF)_2$ in refluxing THF or by the reaction of $[V_2(\mu\text{-}Cl)_3(THF)_6]_2Zn_2Cl_6$ with $ZnCl_2(THF)_2$ in THF at 90 °C. The crystal structure indicates discrete molecules of $(THF)_4V(\mu\text{-}Cl)_2ZnCl_2$. The six-coordinate environment of vanadium approximates octahedral geometry whereas the four-coordinate zinc geometry is virtually tetrahedral. The octahedron and tetrahedron are linked by two chloride bridges. Crystals belong to the monoclinic space group $P2_1/c$ with cell dimensions (−158 °C) a = 14.732 (5) Å, b = 9.680 (3) Å, c = 16.207 (6) Å, and β = 94.12 (2)° and Z = 4. High catalytic activity was found for ethylene polymerization by the title compound as well as for several other related V/Zn/Cl/THF compounds whose structures have been established. Catalyst activity is greatly enhanced by added halocarbons. Activity of V(II) compounds equals or exceeds that of V(III) compounds, which tends to deny a previous suggestion that the halocarbon functions to keep vanadium in oxidation state +3. Moreover, the V(II) compounds fail to be oxidized to V(III) even by neat CH_2Cl_2.

Introduction

Recently groups at Indiana University, Phillips Petroleum, and Texas A&M have independently discovered that the zinc reduction of vanadium trichloride in tetrahydrofuran does not lead to a mixture of $VCl_2(THF)_2$ and $ZnCl_2\cdot x$THF as previously claimed,[1,2] but to a compound containing vanadium and zinc in a 2:1 ratio. This product has been characterized by X-ray crystallography as $[V_2(\mu\text{-}Cl)_3(THF)_6]_2Zn_2Cl_6$.[3,4] Actually, the reaction of vanadium halides with zinc or dialkylzinc in ether solvents is even more complicated than this result indicates, as seen from the work of Thiele et al.[5] Thus, from reactions of vanadium tetrachloride and dimethylzinc, compounds formulated as $2VCl_3\cdot ZnCl_2\cdot 8THF$ and $2VCl_2\cdot ZnCl_2\cdot 6THF$ were reported. The latter material is identical with the dimer mentioned above.

In the area of high-activity Ziegler-Natta catalysts,[6] mixed chlorides of vanadium and zinc are relevant to two questions of current interest. One of these questions involves the oxidation state of vanadium in these catalysts, and the second is concerned with the role of electropositive metals, such as magnesium, in these catalysts. The compounds $[V_2(\mu\text{-}Cl)_3(THF)_6]_2Zn_2Cl_6$ and $[trans\text{-}VCl_2(THF)_2(H_2O)_2]ZnCl_3(THF)$ were characterized by earlier structural studies[3,4,7] while the product $VCl_3\cdot ZnCl_2\cdot 5THF$ was found to be isomorphous and presumably isostructural with $[trans\text{-}TiCl_2(THF)_4]ZnCl_3(THF)$.[8] We continue here with a structural study of $VCl_2\cdot ZnCl_2\cdot 4THF$ and report on the use of these compounds as ethylene-polymerization catalysts.

Experimental Section

General Procedures and Materials. All manipulations were carried out under argon or nitrogen atmosphere with standard Schlenk or drybox techniques. Tetrahydrofuran was dried by refluxing over potassium or Na/K/benzophenone. Anhydrous VCl_3 and VCl_4 were commercial materials while the dimer, $[V_2(\mu\text{-}Cl)_3(THF)_6]_2Zn_2Cl_6$, and $VCl_3\cdot ZnCl_2\cdot 5THF$ were prepared as previously described.[3,7] Powder patterns were recorded with Cu Kα radiation on a Philips Norelco powder diffractometer equipped with a graphite monochromator.

Polymerizations. Polymerization of ethylene was carried out in a stirred 1-gal Autoclave Engineers reactor at 100 °C. The reactor was charged with 1.0 mmol of triethylaluminum, 2.0 mmol of 1,2-difluorotetrachloroethane, about 10 mg of vanadium compound, 2 L of isobutane, and a slight hydrogen pressure. After the mixture was heated to 100 °C, ethylene (the ethylene and isobutane were both Phillips polymerization grade passed over activated alumina) was added so as to increase the total pressure by 15.9 bar, and the pressure was held at this value for 1 h by supplying ethylene on demand. The reactor was finally vented and the polymer removed.

By an increase in the amount of hydrogen added to the reactor, the molecular weight of the polymer could be lowered to the desired value.

[†] Phillips Petroleum Co.

[‡] Indiana University.

(1) Kohler, F. H.; Prossdorf, W. *Z. Naturforsch., B: Anorg. Chem., Org. Chem.* **1977**, *32B*, 1026–1029.

(2) Hall, V. N.; Schmulbach, C. D.; Soby, W. N. *J. Organomet. Chem.* **1981**, *209*, 67–76.

(3) Bouma, R. J.; Teuben, J. H.; Beukema, W. R.; Bansemer, R. L.; Huffman, J. C.; Caulton, K. G. *Inorg. Chem.*, **1984**, *23*, 2715–2718.

(4) Cotton, F. A.; Duraj, S. A.; Extine, M. W.; Lewis, G. E.; Roth, W. J.; Schmulbach, C. D.; Schwotzer, W. *J. Chem. Soc., Chem. Commun.* **1983**, 1377–1378.

(5) Thiele, K. H.; Jacob, von K.; Wagner, S.; Schumann, W. *Z. Anorg. Allg. Chem.* **1976**, *427*, 75–84.

(6) Gavens, P. D.; Bottrill, M.; Kelland, J. W.; McMeeking, J. In "Comprehensive Organometallic Chemistry"; Pergamon Press: New York, 1982; Vol. III, pp 475–547.

(7) Folting, K.; Huffman, J. C.; Bansemer, R. L.; Caulton, K. G.; Martin, J. L.; Smith, P. D. *Inorg. Chem.* **1984**, *23*, 4589.

(8) Folting, K.; Huffman, J. C.; Bansemer, R. L.; Caulton, K. G. *Inorg. Chem.* **1984**, *23*, 3289.